Electronic Supplementary Information for

Role of the Molecular Structure of Carboxylate-Alumoxanes on the Enhanced Nucleation of Polypropylene

Mohanraj Mani,[a] Ramesh Chellaswamy,*[a] Yogesh N. Marathe[a] and Vijayamohanan K. Pillai[b]

[a]Polymer Science and Engineering Division, Polymers and Advanced Materials Laboratory, CSIR-National Chemical Laboratory, Dr. Homi Bhabha Road, Pune 411 008, India.

[b]CSIR-Central Electrochemical Research Institute, Karaikudi 630006, India.

Email: c.ramesh@ncl.res.in

EXPERIMENTAL SECTION

Materials

Aromaticcarboxylic acids were procured from Sigma-Aldrich. Metal nitrates were purchased form Vijay chemicals Ltd, India. Isotactic polypropylene (iPP) homopolymer in the form of powder was kindly supplied by Reliance Industries Ltd., Mumbai. The weight-average molar mass obtained by gel permeation chromatography (GPC) in 1,2,4-trichlorobenzene at 160 °C was found to be Mw = 250 000 with the polydispersity index of Mw/Mn = 4.6.

Methods

Preparation of PTBBA-alumoxane: $Al(NO_3)_3.9H_2O$ was taken in a 500 ml jacketed reactor equipped with an overhead stirrer. Subsequently 225 ml of deionized water was added and the solution was heated to 100 °C. It formed a boehmite gel when the solution pH was adjusted to neutral by 5% of freshly prepared ammonia solution while stirring at 1000 rpm. After 30 mins 75 ml of isopropyl alcohol containing *p-t*-butylbenzoic acid (PTBBA) was added and the reaction mixture was stirred for 2 hrs at 100 °C at 1000 rpm. The white precipitate was separated by centrifugation and washed with methanol. The product was powdered and dried under vacuum at 80 °C for about 12 hrs. The same procedure was followed for the preparation of other carboxylate-alumoxanes and Zirconium-PTBBA complex. The metal nitrate to carboxylic acid molar ratio was maintained at 1:2. $ZrO(NO_3)_2.xH_2O$ salt was used to prepare Zirconium-PTBBA complex.

The NAs were pre-mixed with iPP powder and extruded at 200 °C using a DSM twin-screw micro extruder. The samples were allowed to mix for 2 min in the barrel at 100 rpm screw speed. The crystallization temperature of the nucleated iPP was measured by Differential Scanning Calorimetry TA Q100 in N_2 atmosphere at a purge flow rate of 50 mL/min. About 4-6 mg of sample was heated to 200 °C and held for 2 mins. The melt crystallization temperature, T_C, was the peak crystallization temperature on subsequent cooling. Both the heating and cooling rates were maintained at 10 °C/min.

The WAXS measurements were carried out using a Rigaku Micromax-007HF diffractometer operating at 40 kV and 30 mA. The samples were exposed to the X-ray beam for 3 mins and the scattering pattern was imaged by Rigaku R-AXIS IV++ area detector. The 2D pattern was converted to 1D pattern by Rigaku 2DP software.

TEM images were taken using a Transmission Electron Microscope model FEI Technai G2 T20, Japan. The samples were prepared by dispersing in benzylalcohol and drop casted on to 200 mesh carbon coated copper grids.

The MALDI−TOF analysis was done on AB SCIEX TOF/TOF 5800 (Applied Biosystem, Framingham, USA) equipped with 337 nm pulsed nitrogen laser used for desorption and ionization. The samples were dispersed in benzyl alcohol and premixed with dithranol matrix before spotting onto the 96-well stainless MALDI plate. The samples were thoroughly dried at room temperature before MALDI analysis.

FT-IR spectra with a resolution of 2 cm^{-1} were collected using Perkin-Elmer spectrometer (model Spectrum GX) with samples in KBr pellets.

Table S1: Crystallization temperature (T_C) of iPP (unnucleated) and nucleated with PTBBA-alumoxane and DMDBS on various cooling rate.

Cooling rate (°C/min)	Crystallization temperature (T_C) of iPP (°C)		
	iPP	PTBBA-alumoxane	DMDBS
5	116.6	134.3	132.6
10	112.6	131.6	130.2
20	108.6	129.0	127.2
30	105.4	126.2	124.8
40	104.0	124.2	123.6

S1

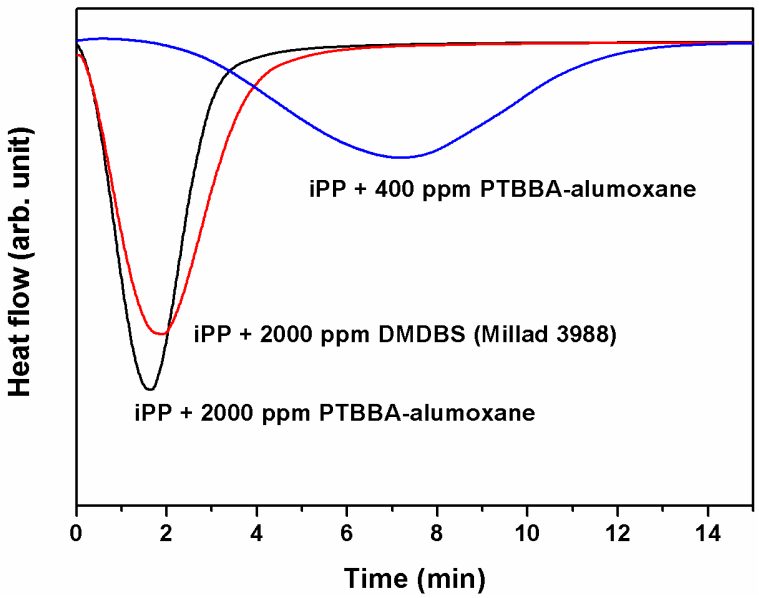

Figure S1. DSC curves of isothermally crystallized iPP with PTBBA-alumoxane and DMDBS at 140 °C. Please note that bare iPP and iPP+400ppm DMDBS samples did not nucleate within this experimental time scale.

S2

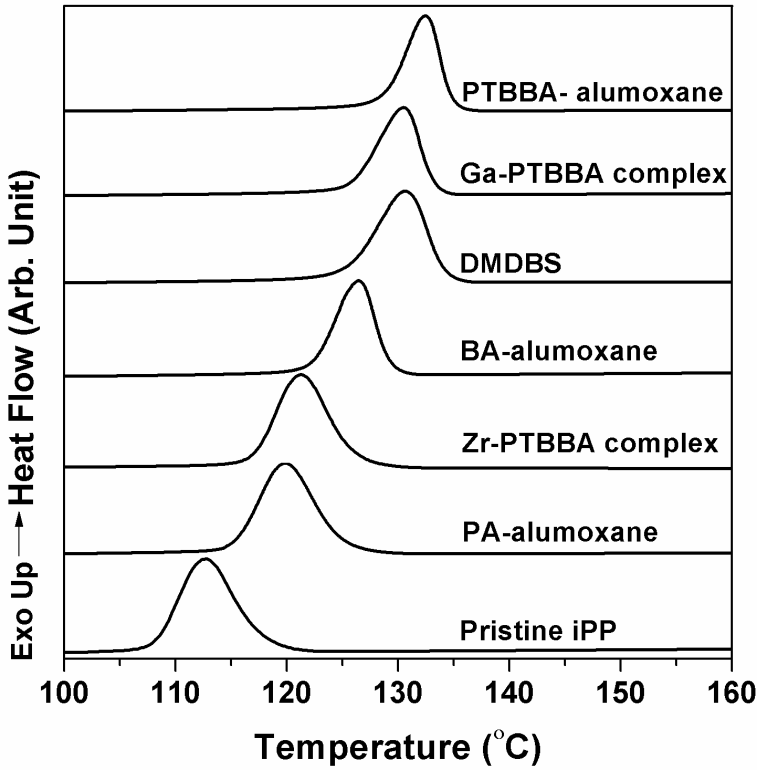

Figure S2. DSC melt crystallization thermograms (cooling cycle) of pristine iPP and iPP nucleated with 2000ppm of various nucleating agents.

S3

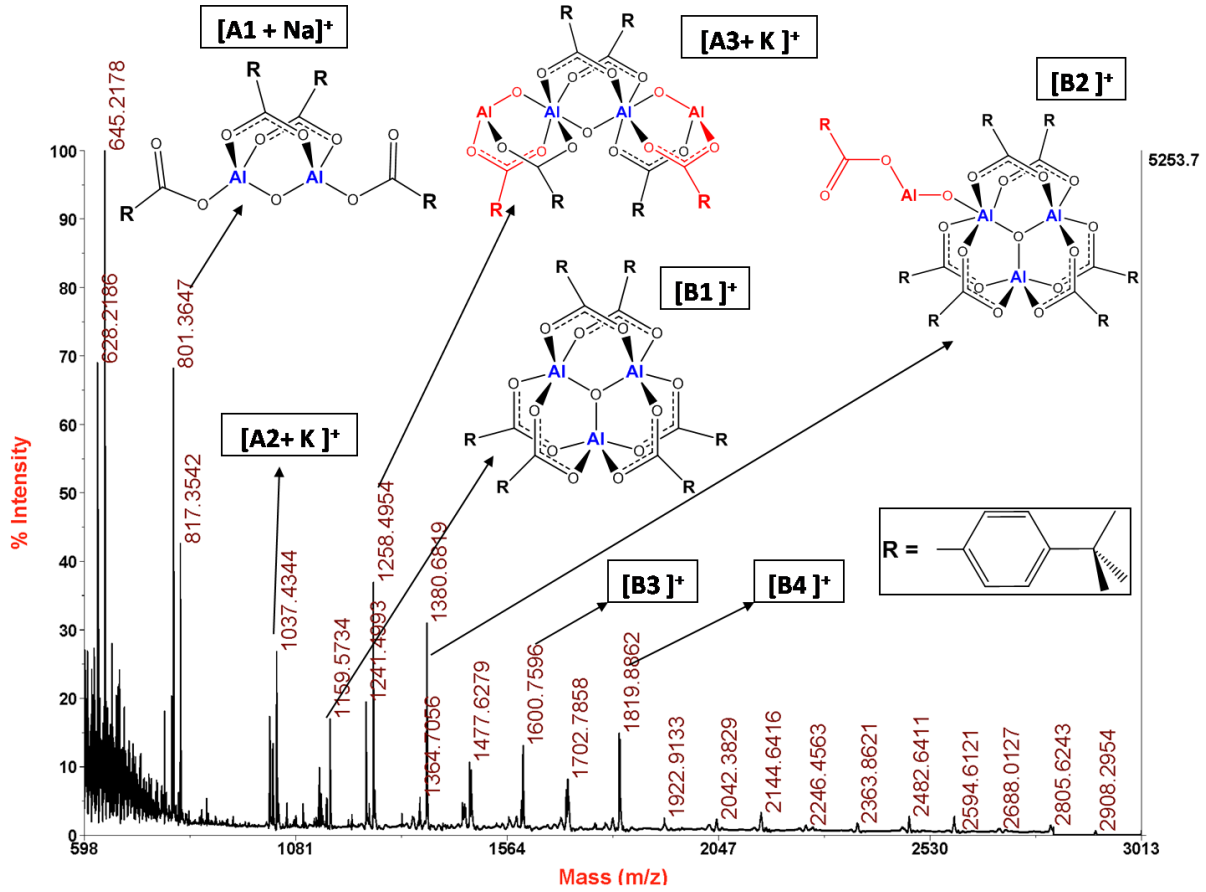

Figure S3. MALDI-TOF/MS of PTBBA-alumoxane

It is also interesting to note that the presence of series of peaks at the regular interval of 220 Da (i.e., 817 Da, 1037 Da, 1258 Da, 1477 Da etc.), indicating that the basic building unit in the higher molecular weight species is O-Al-PTBBA (molecular mass 220 Da). Successive addition of O-Al-PTBBA unit into the dinuclear complex (A1) gives trinuclear (A2), tetranuclear (A3) and pentanuclear (A4) and polynuclear aluminium complexes as shown in Figure S3. This is in excellent accordance with the reported coordination polymer of aluminum 1,4-benzenedicarboxylate (BDC), $Al(OH)(C_8H_4O_4)\cdot 0.7C_8H_6O_4$.[1] Similarly, another series of peaks is observed at 1159 Da, 1380 Da, 1600 Da, 1819 Da etc. corresponding to B1, B2, B3, B4 and like. Notably, these polynuclear complexes are based on oxo-centred trinuclear aluminium core. It seems that water molecules and hydroxyl groups, which would complete the Al coordination sphere, leave the structure during laser ablation process of the MALDI-TOF/MS analysis. Hence the MS analysis gives m/z peaks without such ligands as shown in Figure S3.

S4

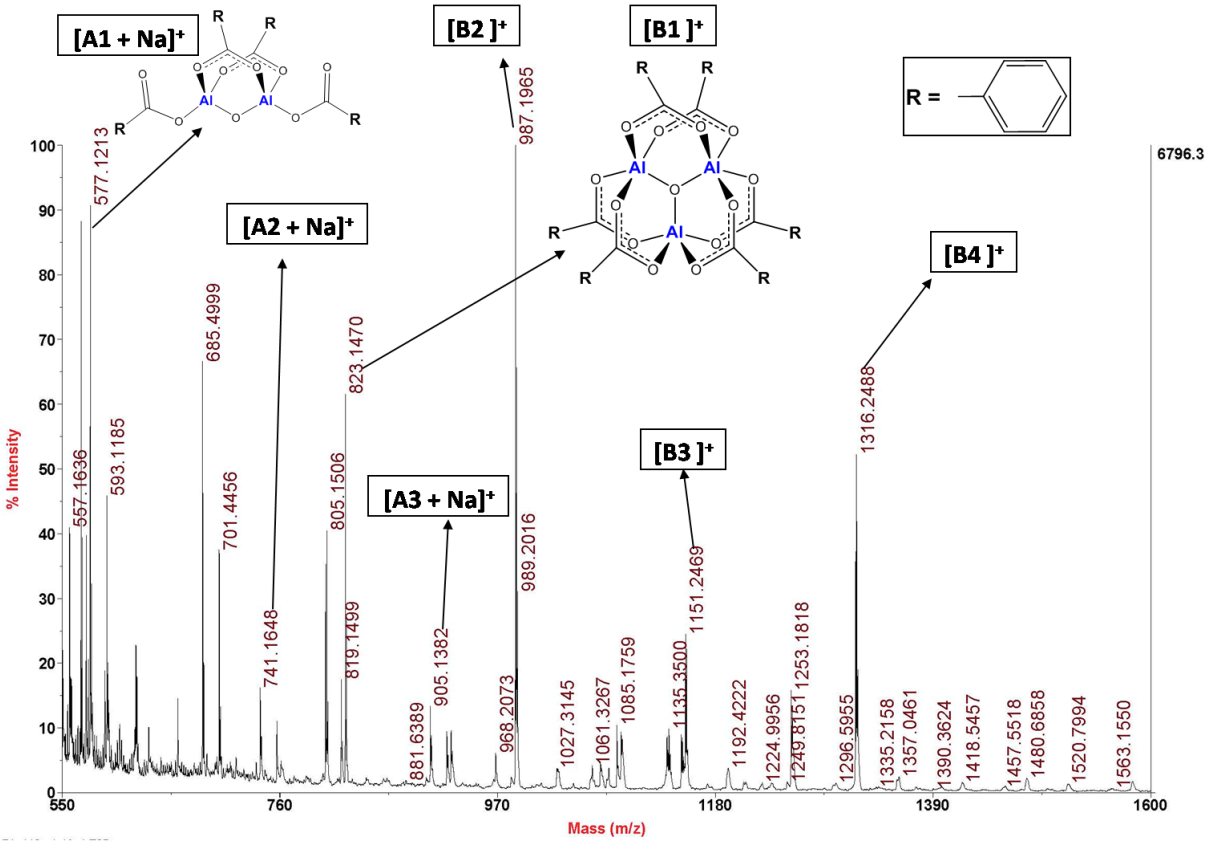

Figure S4. MALDI-TOF/MS of BA-alumoxane

The MALDI-TOF-MS of BA-alumoxane (Figure S4) shows peak at 577 Da corresponding to molecular formula $[(C_6H_4CO_2)Al(\mu\text{-}O)(\mu\text{-}O_2CC_6H_4)]_2$ along with that for Na^+ ion. Like PTBBA-alumoxane, this compound also shows two series of peaks at the regular interval (i.e., 164 Da, molecular mass of O-Al-BA unit) suggesting that the repeating unit in the other higher molecular weight component is [O-Al-BA]. The first series peaks appear at 577 Da, 741 Da and 905 Da, corresponding to A1, A2 and A3. The second series shows peaks at 823 Da, 987 Da, 1151 Da and 1316 Da corresponding to B1, B2, B3 and B4, which are based on oxo-centered trinuclear aluminium core.

S5

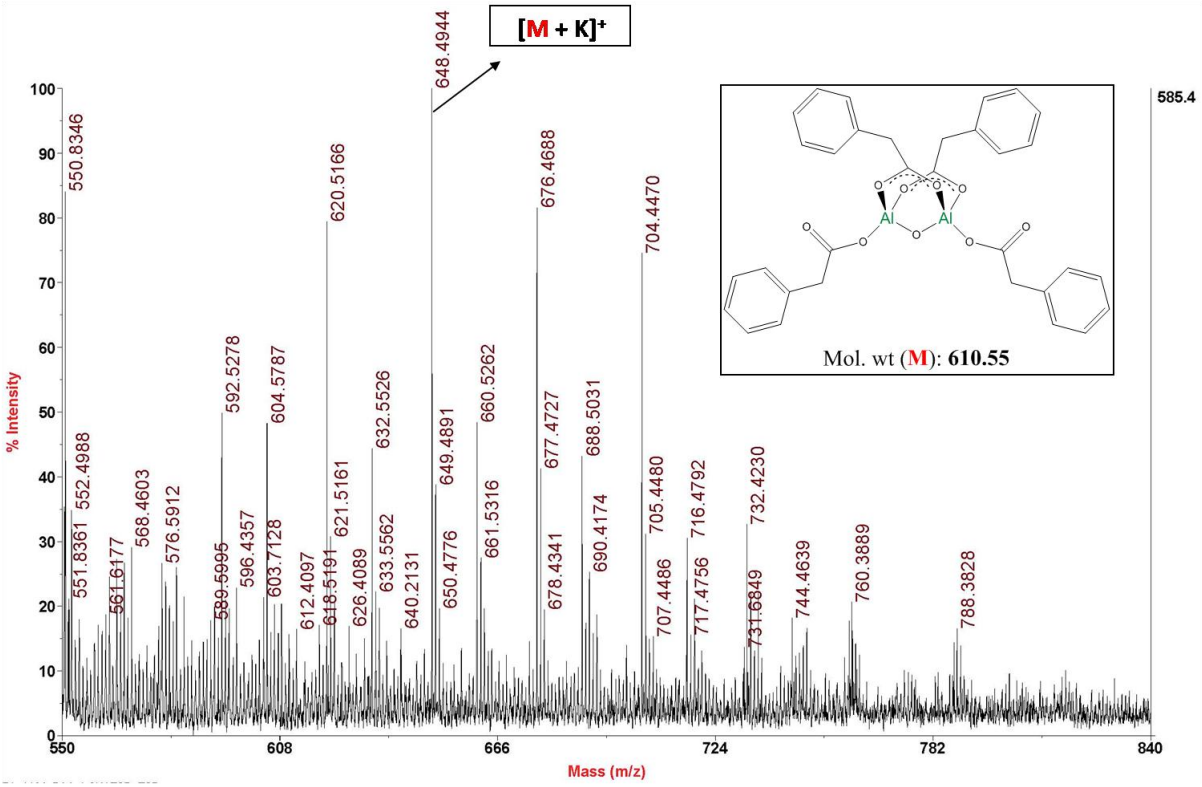

Figure S5. MALDI-TOF/MS of PA-alumoxane

Figure S5 shows the MALDI-TOF-MS of PA-alumoxane and the peaks at m/z at 648 Da corresponding to dinuclear aluminium complex with the molecular formula $[(C_6H_4CH_2CO_2)Al(\mu\text{-}O)(\mu\text{-}O_2C\ CH_2C_6H_4)]_2$ along with that for K^+ ion.

S6

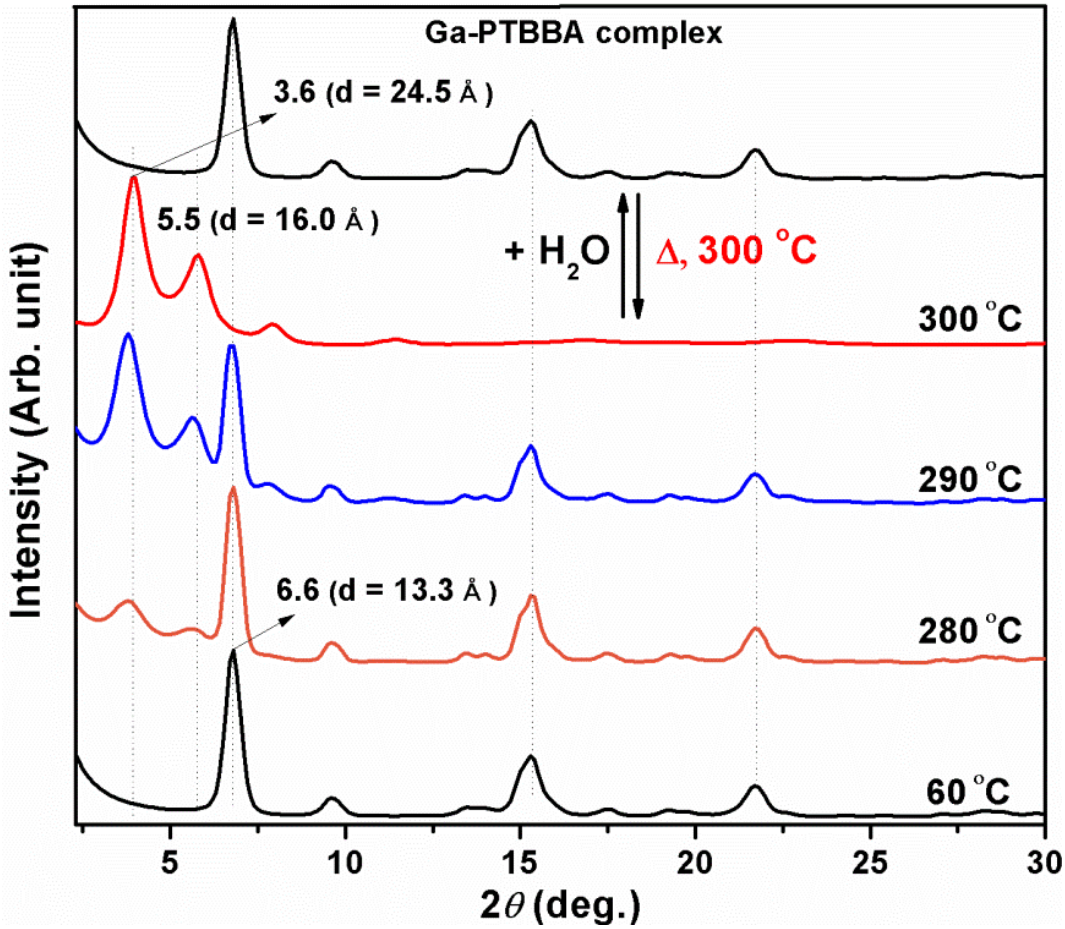

Figure S6. WAXS pattern of Ga-PTBBA and of its annealed samples

S7

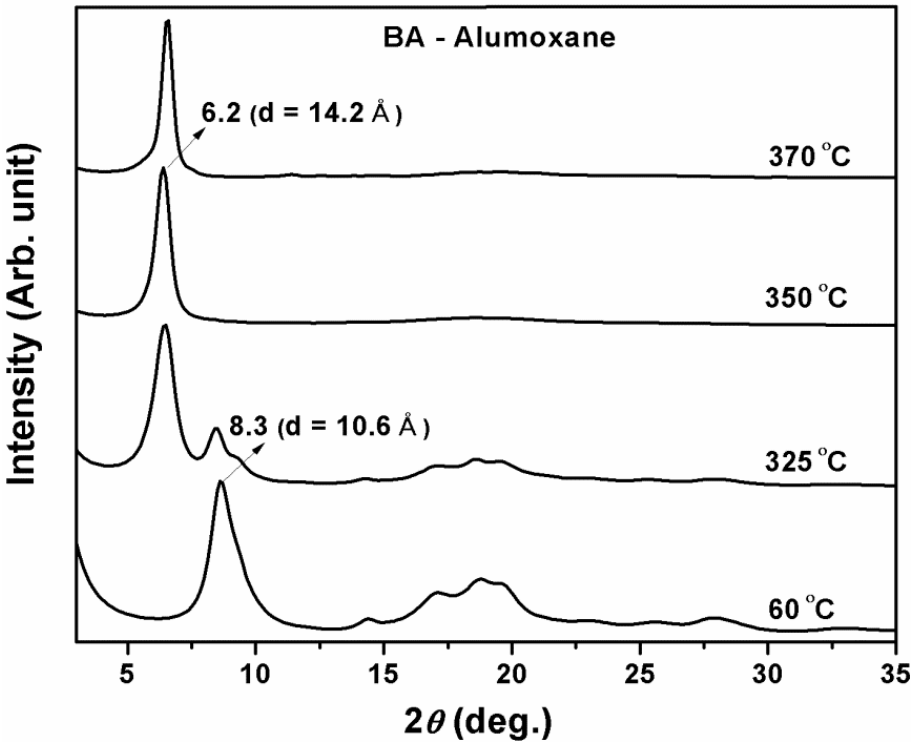

Figure S7. WAXS pattern of BA-alumoxane and of its annealed samples

S8

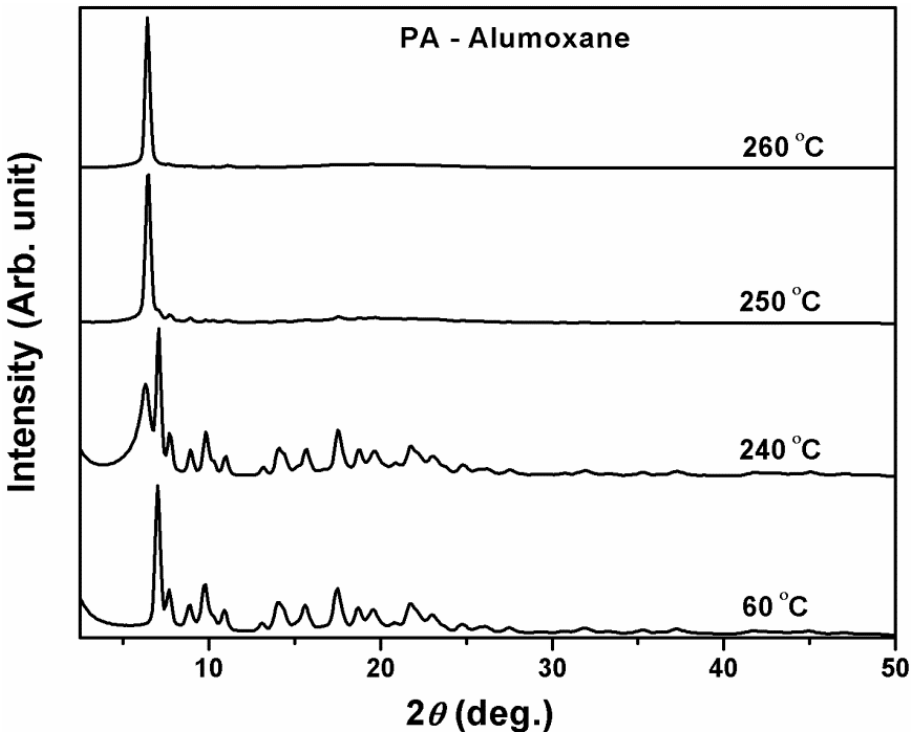

Figure S8. WAXS pattern of PA-alumoxane and of its annealed samples

S9

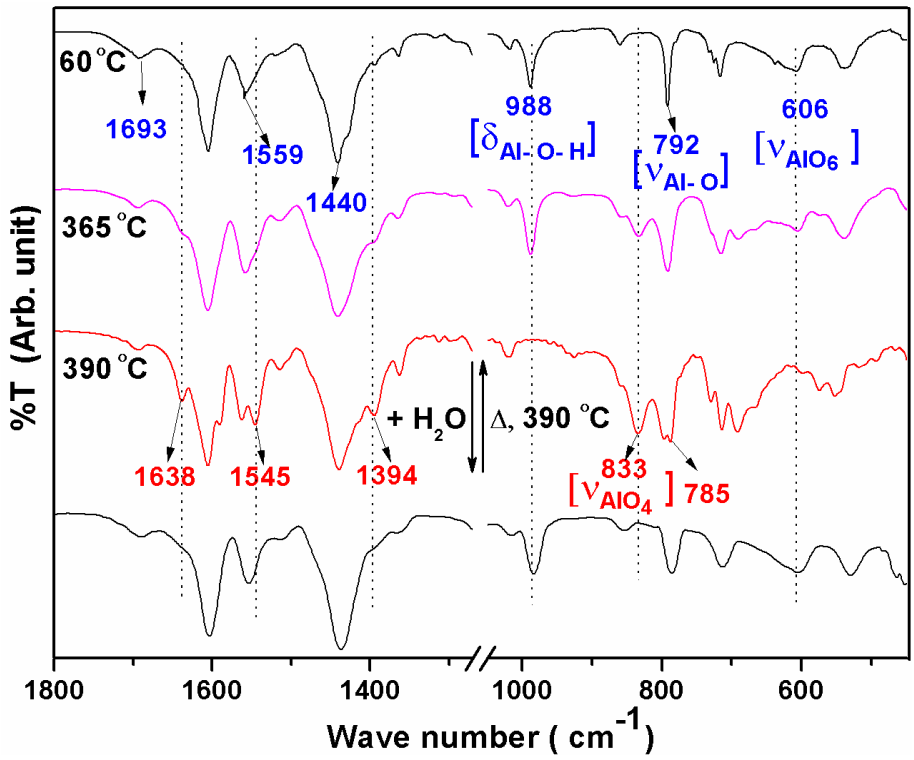

Figure S9. FT-IR spectra of PTBBA-alumoxane annealed at different temperatures (indicated in graph) and scanned at room temperature.

The FT-IR spectrum of PTBBA-alumoxane is shown in Fig. S9. The asymmetric (vas) and symmetric (vs) COO^- stretching vibrations occur at 1559 cm^{-1} and 1440 cm^{-1} respectively, which are characteristic of bridged bidentate coordination.[2] The peak at 1693 cm^{-1} corresponds to C=O stretching indicating the presence of unidentate PTBBA ligand in the product. The Al-O-H stretching and bending modes are observed at 3696 cm^{-1} and 988 cm^{-1} respectively.[3] As discussed in WAXS data, the compound transforms into another crystalline phase at 390 °C and the corresponding FT-IR spectrum is also shown in Fig. S9. FT-IR spectrum shows significant molecular level changes in the transformed material. For example, the 606 cm^{-1} peak assigned to AlO_6 is partly masked while couple of new peaks appear at 833 cm^{-1} and 785 cm^{-1} and are assigned to AlO_4 stretching.[3] Concomitantly Al-O-H stretching and bending peaks at 3696 cm^{-1} and 988 cm^{-1} are vanished indicating dehydroxylation. In addition, another set of new peaks, characteristic of µ-COO- group is observed at 1638 cm^{-1}, 1545 cm^{-1} and 1394 cm^{-1} which are consistent with peak positions of the reported complex [$(Me_3Si)_3$-CAl(µ-O)(µ-Hdtbsa)]2 where the carboxylate group bridges the tetrahedral aluminium centre along with oxo ligand.[4] This spectral change suggests that AlO_6 gets converted into AlO_4 by the removal of coordinated water molecules and hydroxyl groups.

S10

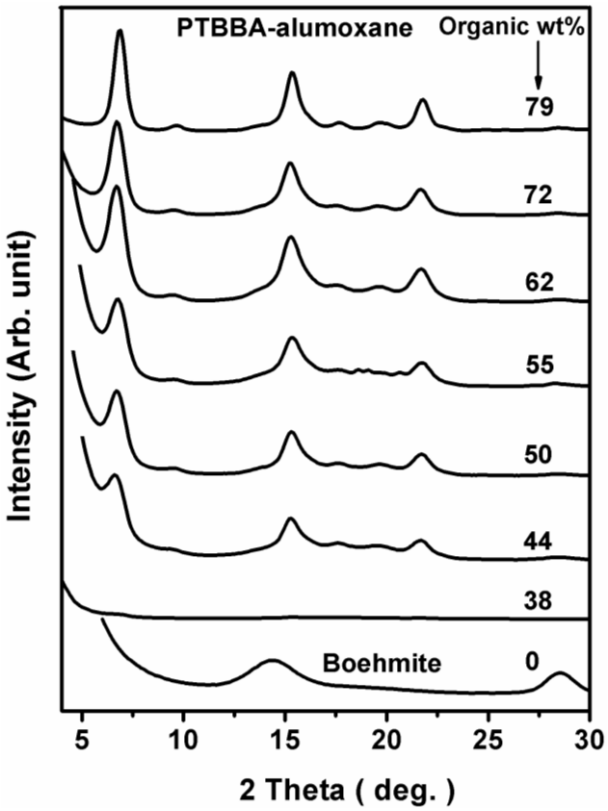

Figure S10. The WAXS pattern of PTBBA-alumoxane with various % of organic content (indicated in graph).

PTBBA-alumoxane with different % of organic content was prepared by varying the Al/PTBBA molar ratio (3.0, 2.5, 2.0, 1.5, 1.0, 0.7 & 0.5). PTBBA-alumoxane shows amorphous pattern when the organic content is about 38%. The nucleation efficiency studies show that the T_C increases upon increase in organic content of PTBBA-alumoxane. The variation of organic content of PTBBA-alumoxane on T_C is shown in Figure S11.

S11

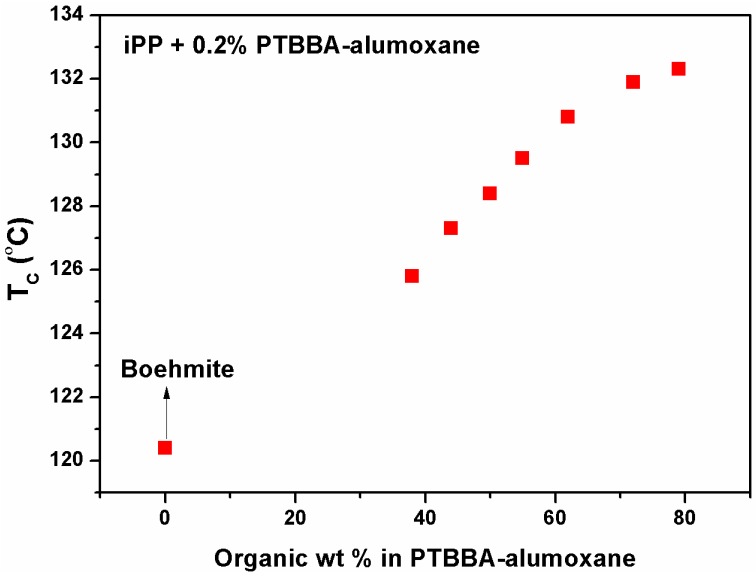

Figure S11. The variation of organic content of PTBBA-alumoxane on T_C.

S12

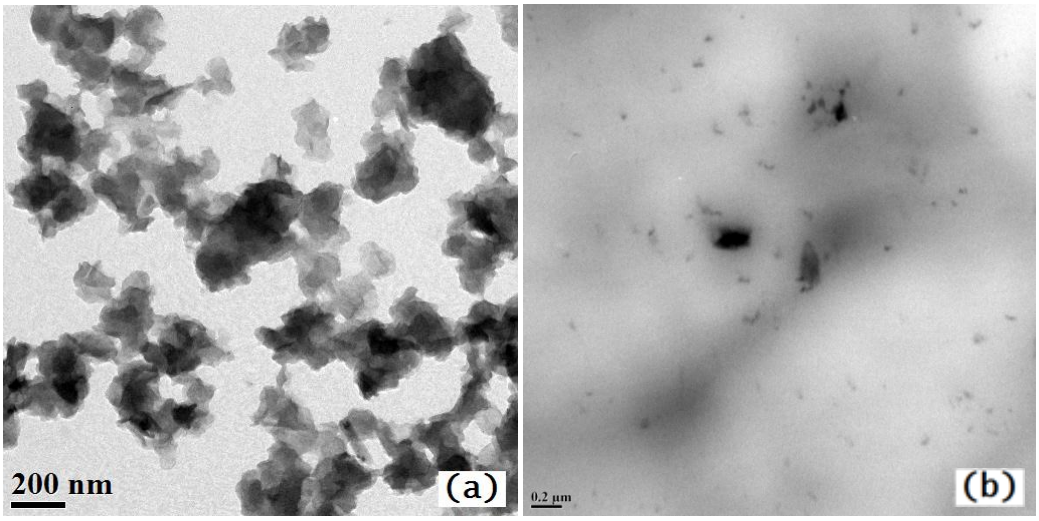

Figure S12. TEM image of BA-alumoxane (a) before and (b) after dispersion in iPP matrix

S13

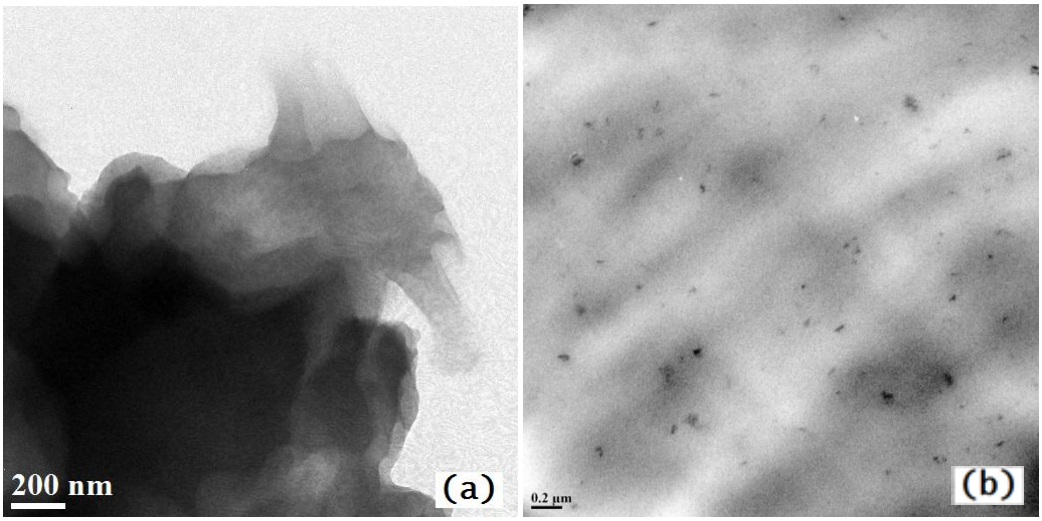

Figure S13. TEM image of PA-alumoxane (a) before and (b) after dispersion in iPP matrix

S14

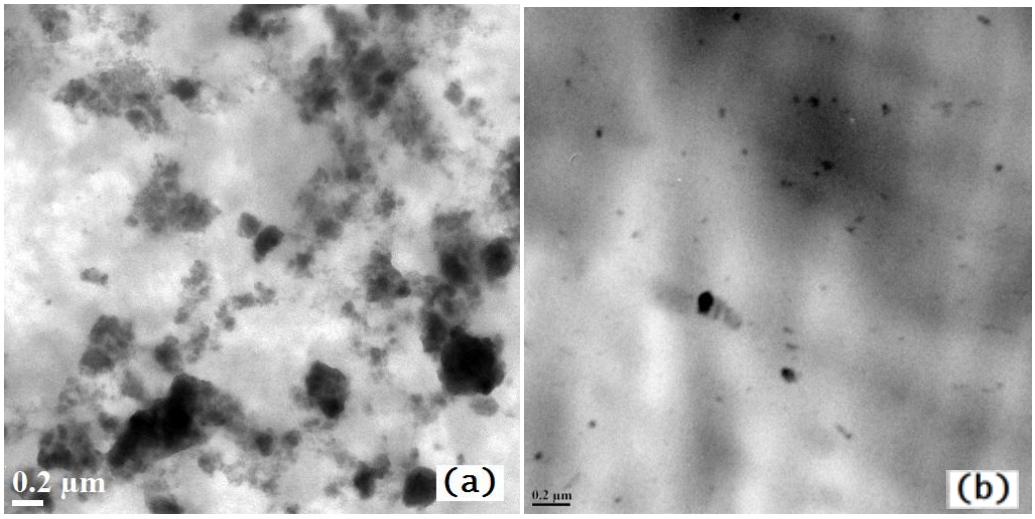

Figure S14. TEM image of Zr-PTBBA particles (a) before and (a) after dispersion in iPP matrix

S15. Nucleation Efficiency Study

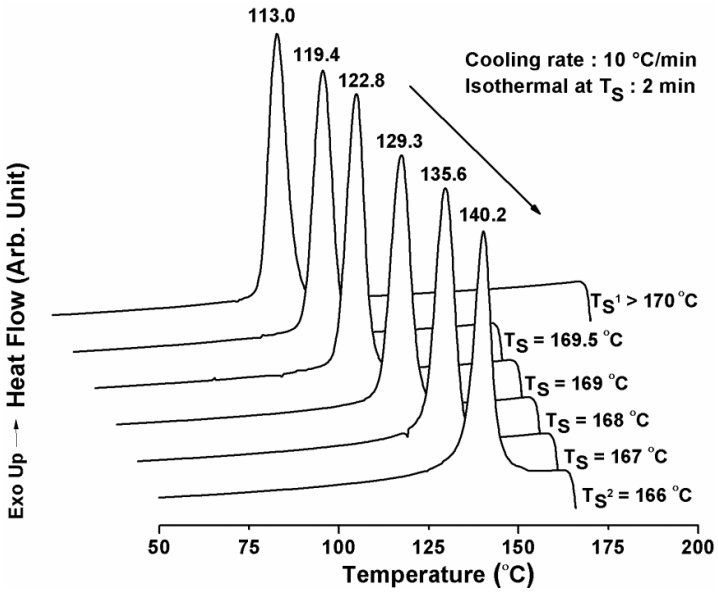

Figure S15. DSC thermogram (cooling cycle) of pristine iPP melt at different self-nucleation temperature (T_S).

S16

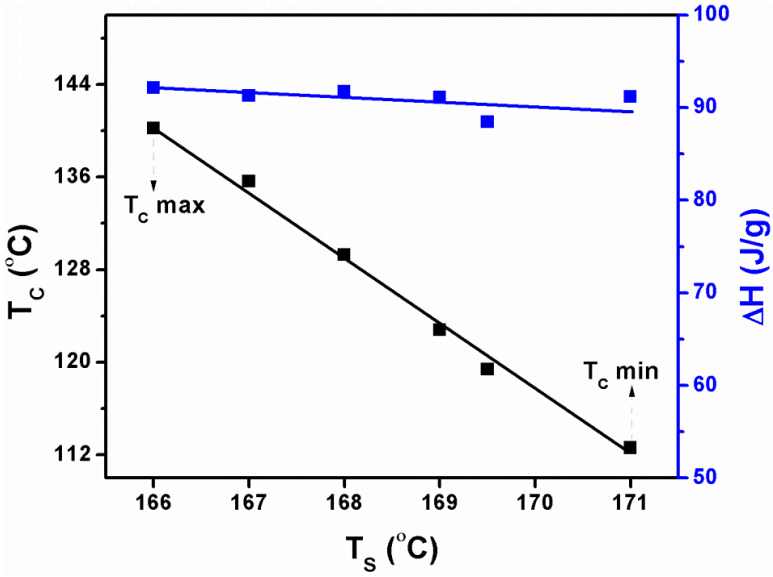

Figure S16. Plot of self-nucleation temperature (T_S) vs. crystallization temperature (T_C) of iPP

The nucleation efficiency (NE) can be calculated as,

$$\mathrm{NE} = 100\,\frac{\mathrm{Tc\,NA} - \mathrm{Tc\,min}}{\mathrm{Tc\,max} - \mathrm{Tc\,min}}$$

T_C NA- Crystallization temperature of the nucleated polymer

T_C min- Lowest crystallization temperature of the pristine polymer obtained from DSC curve T_S1

T_C max- Highest crystallization temperature of the pristine polymer obtained from DSC curve T_S2

S17

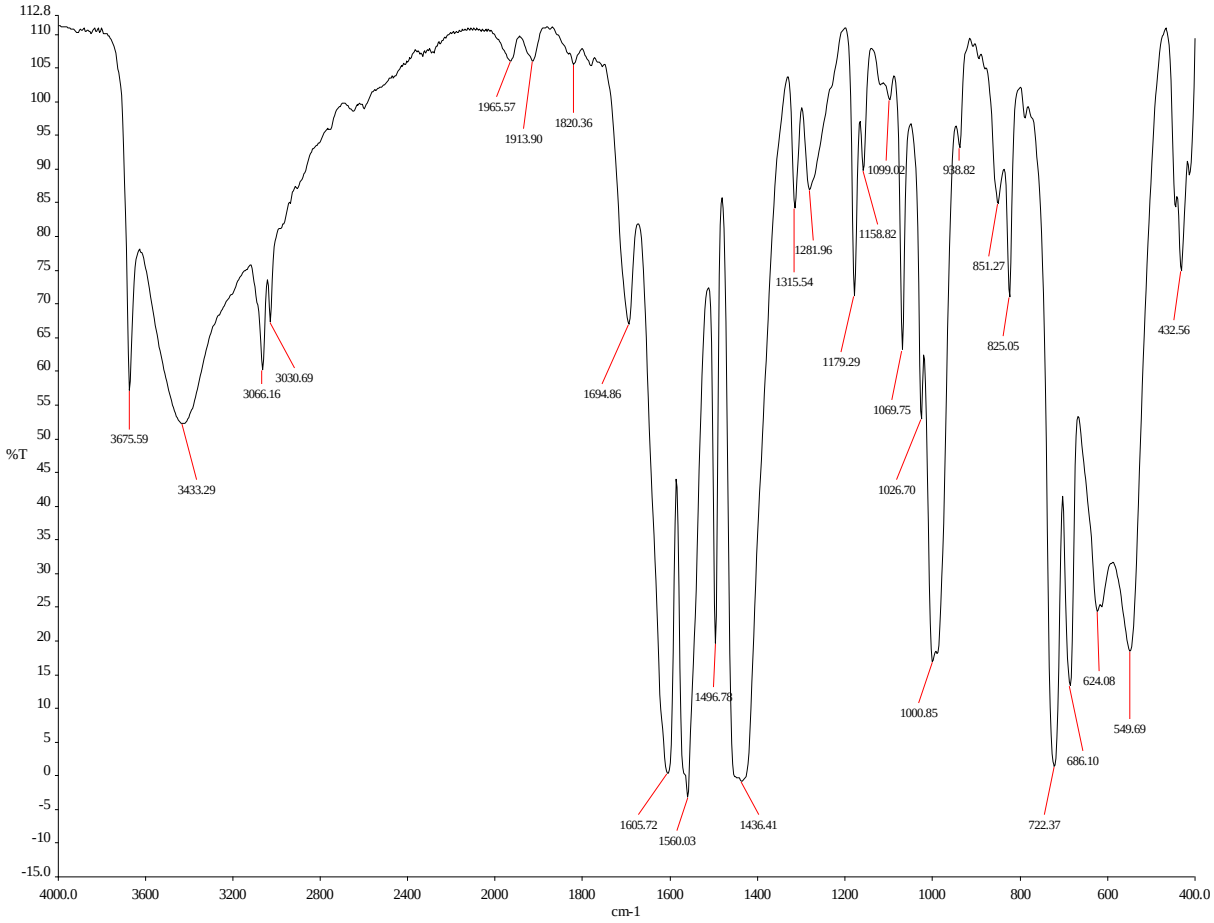

Figure S17. FT-IR spectrum of BA-alumoxane

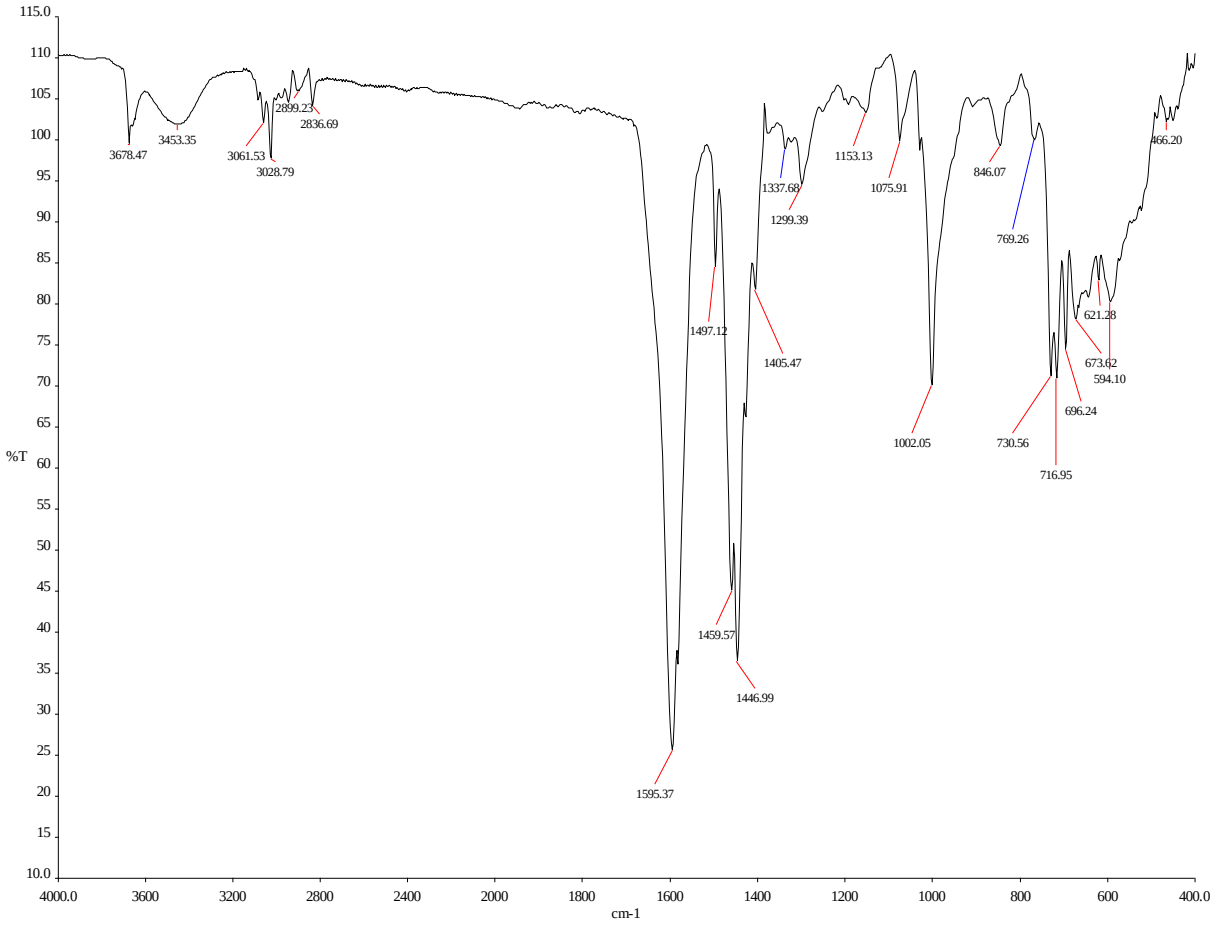

Figure S18. FT-IR spectrum of PA-alumoxane

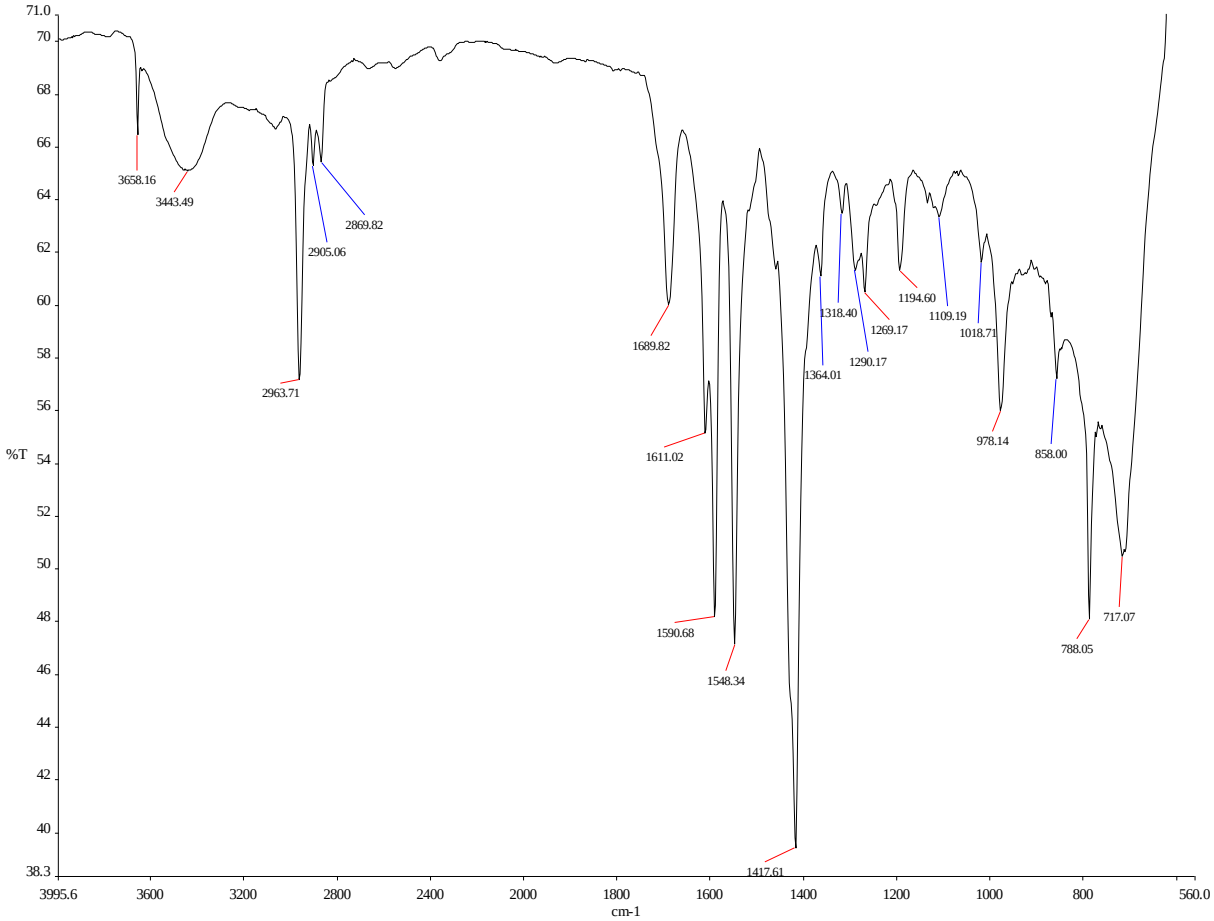

Figure S19. FT-IR spectrum of Ga-PTBBA complex

S20

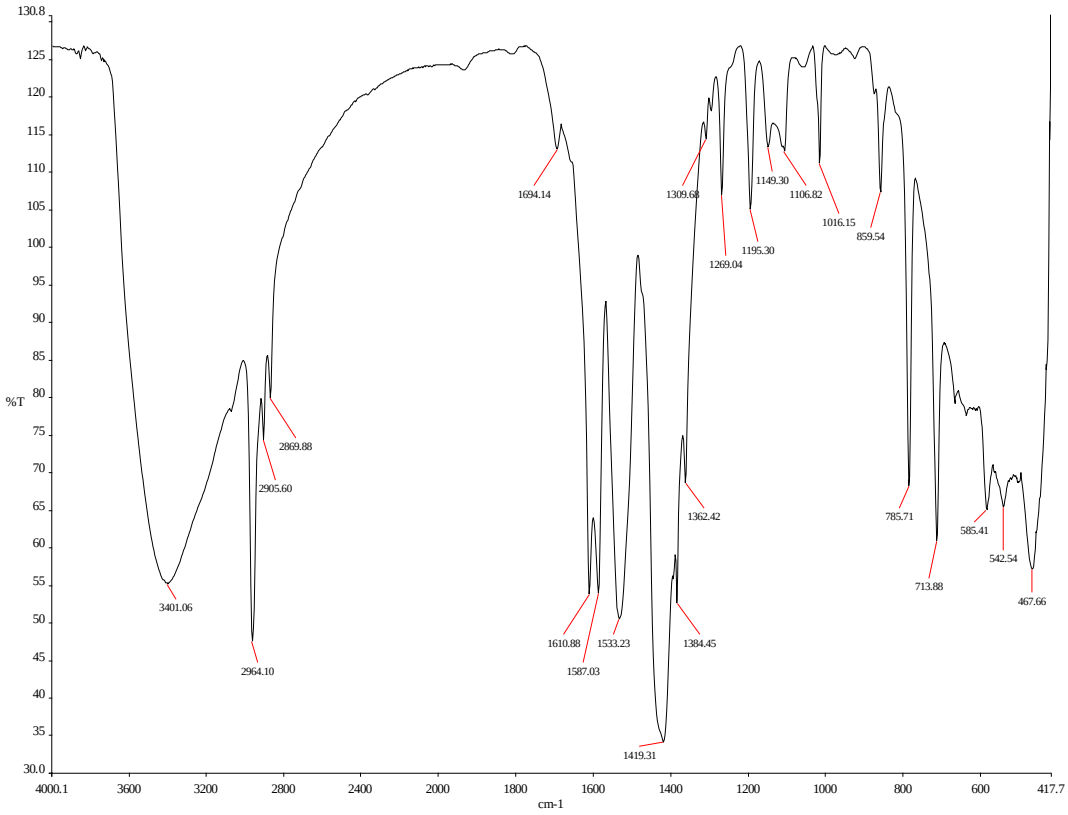

Figure S20. FT-IR spectrum of Zr-PTBBA complex

S21

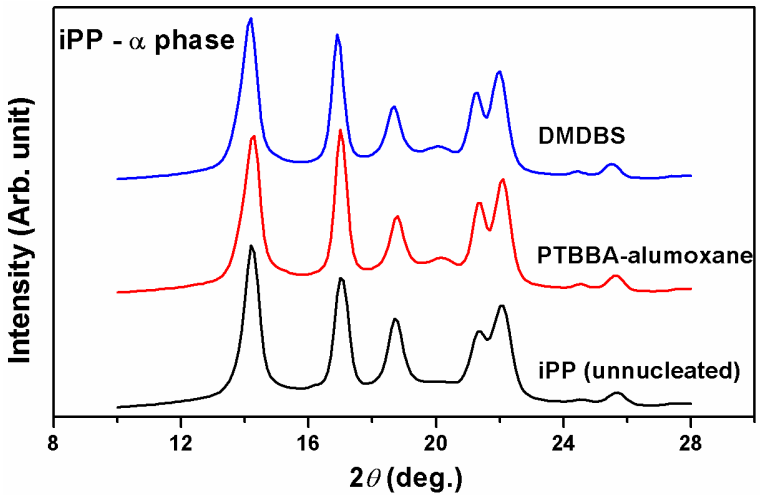

Figure S21. The WAXS patterns of iPP (unnucleated) and nucleated with PTBBA-alumoxane and DMDBS. All the samples have identical processing history. The extruded samples were heated to 210 °C and crystallized on controlled cooling at 10 °C/min.

S22. DFT details

All DFT calculations were performed using the Turbomole 6.4 suite of programs.[5] Geometry optimizations were performed using the Perdew, Burke, and Ernzerhof density functional (PBE).[6] The electronic configuration of the atoms was described by a triple-ζ basis set augmented by a polarization function (Turbomole basis set TZVP).[7] The resolutions of identity (RI)[8] along with the multipole accelerated resolution of identity (marij)[9] approximations were employed for an accurate and efficient treatment of the electronic Coulomb term in the density functional calculations. Single point calculations were made with the hybrid B3-LYP functional [10, 11] in order to obtain more reliable energy values for the different molecular structures.

(1) Vougo-Zanda, M.; Huang, J.; Anokhina, E.; Wang, X.; acobson, A. *J. Inorg. Chem.* 2008, **47**, 11535–11542.

(2) C. Landry, N. Pappe, M. Mason, A. Apblett, A. Tyler, A. MacInnes, and A. Barron, *J. Mat. Chem.,* 1995, **5**, 331-341.

(3) G. K. Priya, P. Padmaja, K. G. K. Warrier, A. D. Damodaran, G. J. Aruldhas, *J. Mater. Sci. Lett.* 1997, **16**, 1584-1587.

(4) L. Kalita, R. Pothiraja, V. Saraf, M. Walawalkar, R. Butcher, and R. Murugavel, *J. Organomet. Chem.,* 2011, **696**, 3155-3161.

(5) Ahlrichs, R.; Bär, M.; Häser, M.; Horn, H.; Kölmel, C. Electronic structure calculations on workstation computers: The program system turbomole. *Chem. Phys. Lett.* 1989, **162 (3),** 165−169.

(6) Perdew, J. P.; Burke, K.; Ernzerhof, M. Generalized Gradient Approximation Made Simple. *Phys. Rev. Lett.* 1996, **77** (18), 3865.

(7) Scha¨fer, A.; Horn, H.; Ahlrichs, R. *J. Chem. Phys.* 1992, **97**, 2571–2577.

(8) Eichkorn, K.; Treutler, O.; Oٌhm, H.; Häser, M.; Ahlrichs, R. Auxiliary basis sets to approximate Coulomb potentials. *Chem. Phys. Lett.* 1995, **240 (4)**, 283−289.

(9) Sierka, M.; Hogekamp, A.; Ahlrichs, R. Fast evaluation of the Coulomb potential for electron densities using multipole accelerated resolution of indentity approximation. *J. Chem. Phys.* 2003, **118**, 9136.

(10) Becke, A. D. *J. Chem. Phys.* 1993, ***98***, 5648.

(11) Lee, C.; Yang, W.; Parr, R. G. *Phys. Rev. B.* 1988, ***37***, 785.